

Electronic supplementary information

Catalytic selective oxidation of isobutane over $\text{Cs}_x(\text{NH}_4)_{3-x}\text{HPMo}_{11}\text{VO}_{40}$ mixed salts

Fangli JING, Benjamin KATRYNIOK, Franck DUMEIGNIL, Elisabeth BORDES-RICHARD
and Sébastien PAUL*,

Index

1. Experimental	2
2. Results	2
2.1. Raman spectroscopy	2
2.2. FT-IR for the used catalysts.....	3
2.3. XRD for the spent catalysts	4
2.4. Nitrogen physisorption	4
2.5. Acidity determined by NH_3 -TPD	5
References.....	6

1. Experimental

Raman spectra were measured on a Jobin-Yvon LabRam Infinity apparatus equipped with a CCD detector operating at liquid nitrogen temperature. A D2 filter was used to protect the catalyst structure from destruction by the laser (wavelength $\lambda=520$ nm). The Raman shift was recorded in the range of 200-1400 cm^{-1} . The homogeneity of the samples was checked by performing the analysis on at least 3 different locations for each sample.

2. Results

2.1. Raman spectroscopy

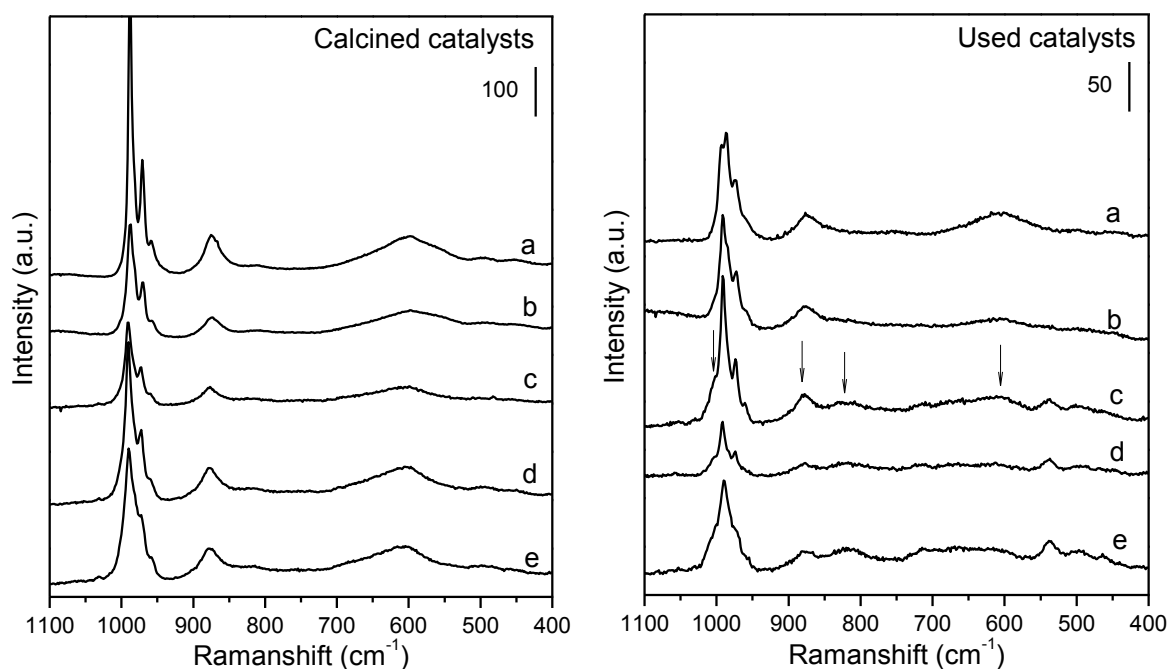


Fig. S1 Raman spectra of the calcined (left) and the used catalysts (right) (a: $\text{Cs}_3(\text{NH}_4)_0\text{H}$, b: $\text{Cs}_{2.5}(\text{NH}_4)_{0.5}\text{H}$, c: $\text{Cs}_{1.7}(\text{NH}_4)_{1.3}\text{H}$, d: $\text{Cs}_{1.5}(\text{NH}_4)_{1.5}\text{H}$, e: $\text{Cs}_{0.5}(\text{NH}_4)_{2.5}\text{H}$). Arrow indicated the MoO_3 phases.

Raman spectroscopy is an effective method to identify the Keggin structure. The Raman features of the catalysts before and after the catalytic reaction were also studied in order to gain more information about the structural evolution during the reaction, and the collected spectra were displayed in Fig. S1. The spectra of the calcined catalysts clearly displayed the Raman characteristic bands from Keggin units: the vibrations at 987, 972, 958, 875 and 600 cm^{-1} were assigned to the $\nu_s \text{Mo}=\text{O}_d$, $\nu_{as} \text{Mo}=\text{O}_d$, $\nu_{as} \text{P}-\text{O}$, $\nu_{as} \text{Mo}-\text{O}_b-\text{Mo}$ and $\nu_{as} \text{Mo}-\text{O}_c-\text{Mo}^1$, respectively. Evident changes could be observed from the Raman spectra for the used samples. Firstly the spectrum for each used sample became less intense compared to the calcined samples. Secondly the peaks shape became much broader especially for the bands from 930 to 1050 cm^{-1} , which

was caused by the reorganization of the structure to give the defective Keggin units. These changes are confirmed by the additional bands appeared at 817, 660 and 537 cm^{-1} most probably resulting from the ill-defined MoO_3 in $\text{Cs}_{1.7}(\text{NH}_4)_{1.3}\text{H}$, $\text{Cs}_{1.5}(\text{NH}_4)_{1.5}\text{H}$, $\text{Cs}_{0.5}(\text{NH}_4)_{2.5}\text{H}$ samples.

Mestl *et al.*² have reported the thermal transition of the unsupported $\text{H}_4\text{PMo}_{11}\text{VO}_{40}$: the vanadyl and molybdenyl were expelled from the Keggin unit to form the defective Keggin structure which further disintegrated to generate Mo_3O_{13} triads. The Mo_3O_{13} triads degraded to more stable end product MoO_3 . While in the used $\text{Cs}_3(\text{NH}_4)_0\text{H}$ and $\text{Cs}_{2.5}(\text{NH}_4)_{0.5}\text{H}$ samples, the three additional bands can not be seen any more. In the catalysts with higher Cs atom number ($x=3$ and 2.5), the structural reorganization was restricted. This is in good agreement with the IR results. On the other hand, the Raman results do not give any information about the V species or the reduction of MoO_3 .

2.2. FT-IR for the used catalysts

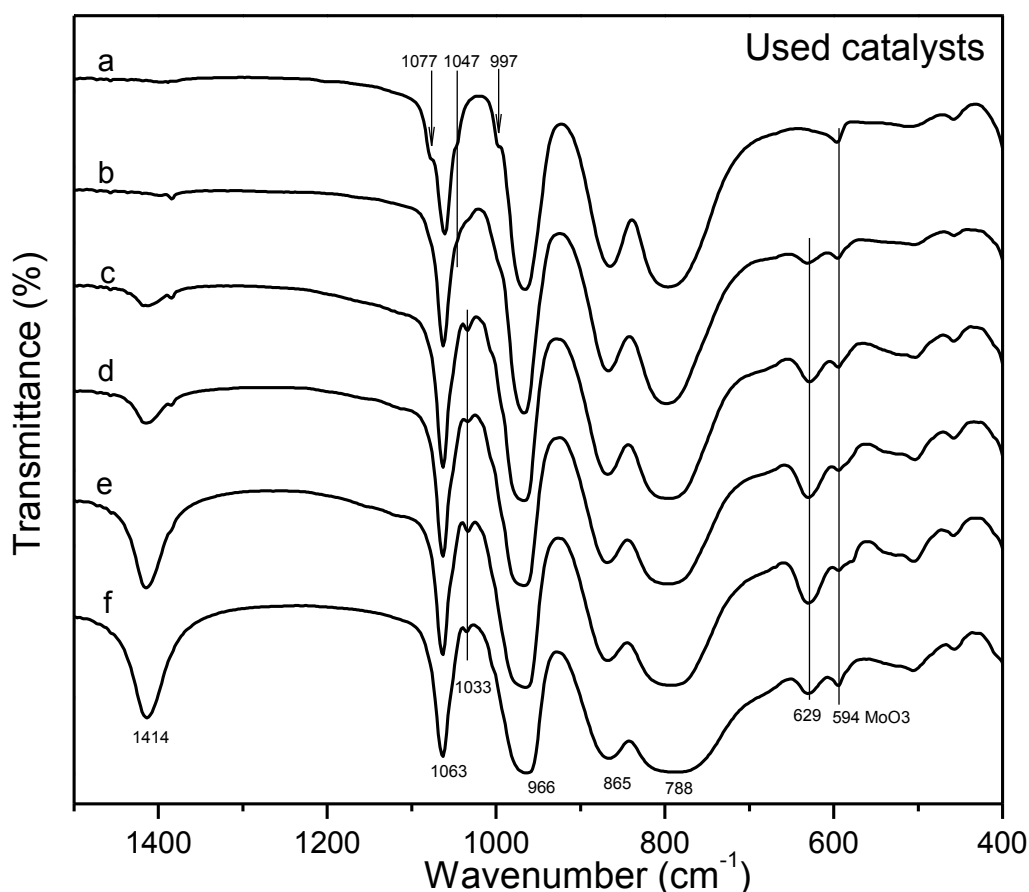


Fig. S2 FT-IR spectra of the spent catalysts [a: $\text{Cs}_3(\text{NH}_4)_0\text{H}$, b: $\text{Cs}_{2.5}(\text{NH}_4)_{0.5}\text{H}$, c: $\text{Cs}_{1.7}(\text{NH}_4)_{1.3}\text{H}$, d: $\text{Cs}_{1.5}(\text{NH}_4)_{1.5}\text{H}$, e: $\text{Cs}_{0.5}(\text{NH}_4)_{2.5}\text{H}$, f: APMV].

2.3. XRD for the spent catalysts

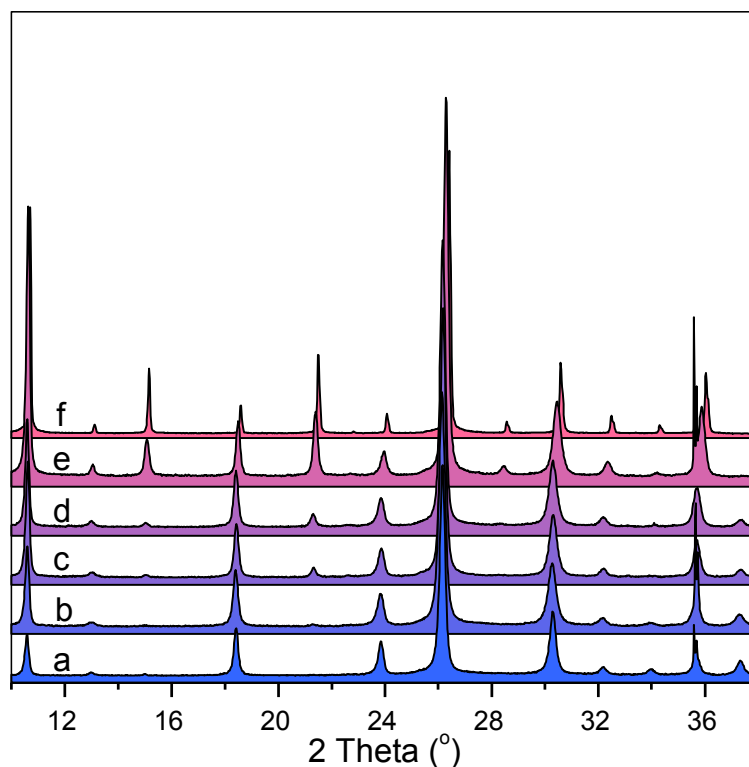


Fig. S3 XRD patterns of the spent catalysts (a: $\text{Cs}_3(\text{NH}_4)_0\text{H}$, b: $\text{Cs}_{2.5}(\text{NH}_4)_{0.5}\text{H}$, c: $\text{Cs}_{1.7}(\text{NH}_4)_{1.3}\text{H}$, d: $\text{Cs}_{1.5}(\text{NH}_4)_{1.5}\text{H}$, e: $\text{Cs}_{0.5}(\text{NH}_4)_{2.5}\text{H}$, f: APMV)

2.4. Nitrogen physisorption

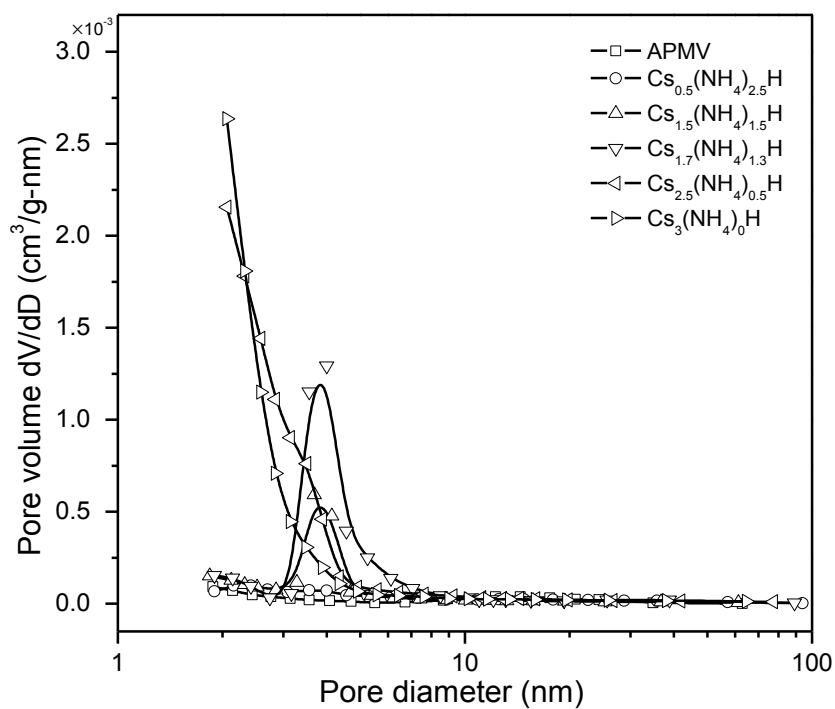


Fig. S4 Pore size distribution of the different calcined samples

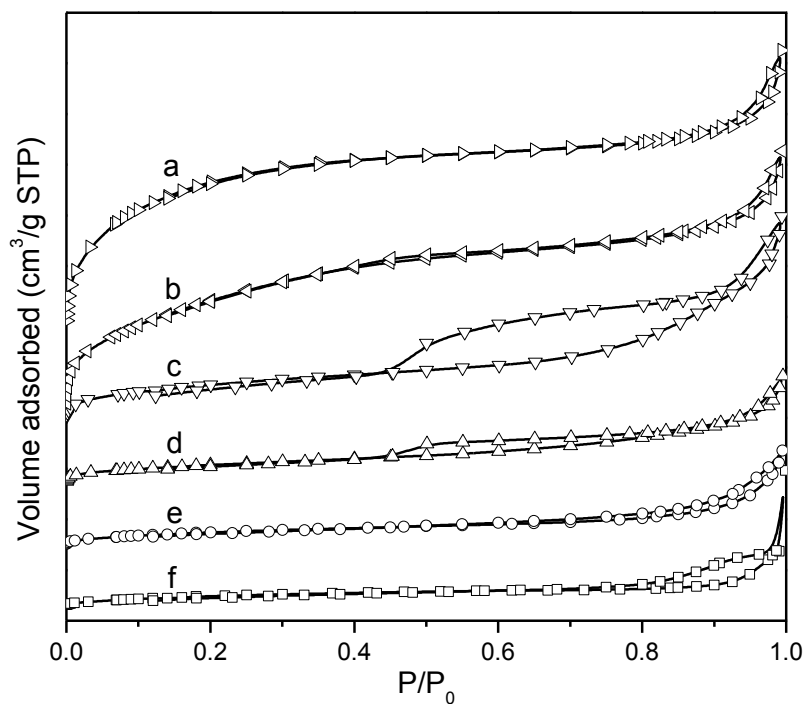


Fig. S5 The isotherms of the different catalysts (a: $\text{Cs}_3(\text{NH}_4)_0\text{H}$, b: $\text{Cs}_{2.5}(\text{NH}_4)_{0.5}\text{H}$, c: $\text{Cs}_{1.7}(\text{NH}_4)_{1.3}\text{H}$, d: $\text{Cs}_{1.5}(\text{NH}_4)_{1.5}\text{H}$, e: $\text{Cs}_{0.5}(\text{NH}_4)_{2.5}\text{H}$, f: APMV)

2.5. Acidity determined by NH_3 -TPD

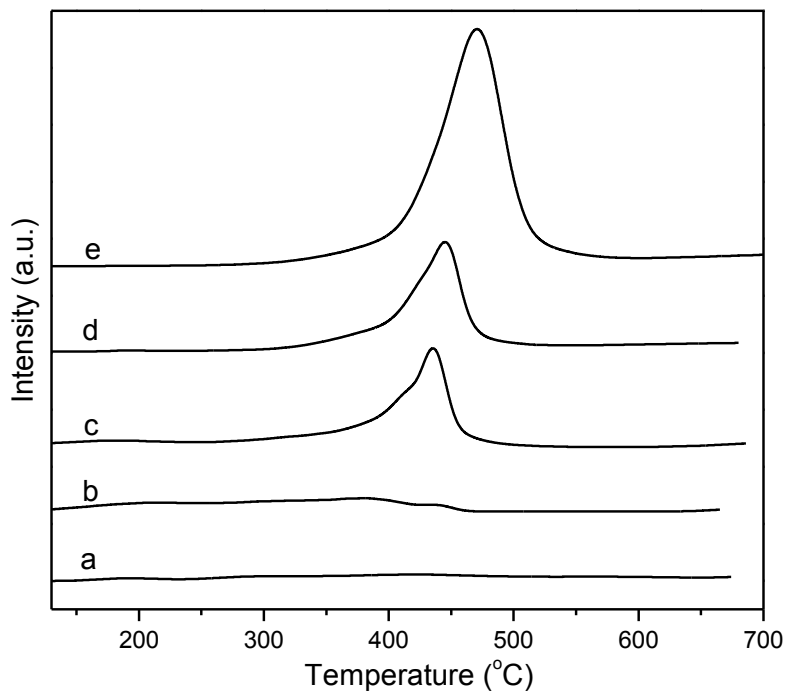


Fig. S6 NH_3 -TPD profiles of the mixed salts (a: $\text{Cs}_3(\text{NH}_4)_0\text{H}$, b: $\text{Cs}_{2.5}(\text{NH}_4)_{0.5}\text{H}$, c: $\text{Cs}_{1.7}(\text{NH}_4)_{1.3}\text{H}$, d: $\text{Cs}_{1.5}(\text{NH}_4)_{1.5}\text{H}$, e: $\text{Cs}_{0.5}(\text{NH}_4)_{2.5}\text{H}$)

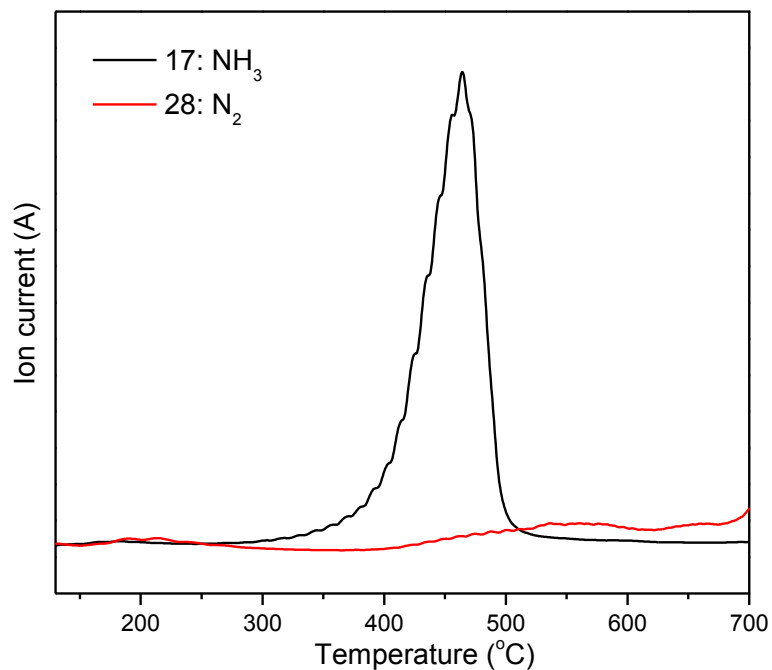


Fig. S7 Mass signal of N_2 and NH_3 during the NH_3 -TPD measurement [sample: $\text{Cs}_{0.5}(\text{NH}_4)_{2.5}\text{H}$]

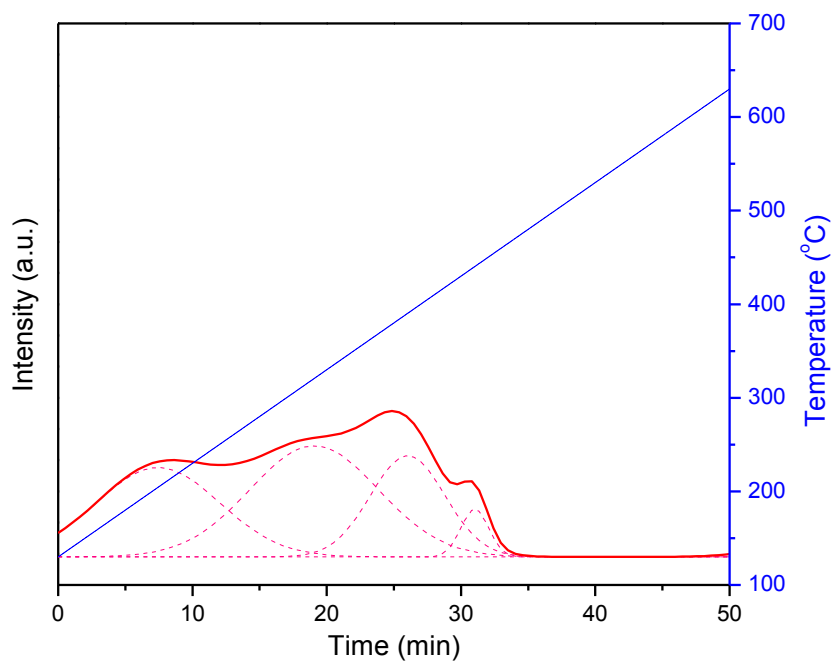


Fig. S8 Peak area integration by deconvolution treatment [sample: $\text{Cs}_{2.5}(\text{NH}_4)_{0.5}\text{H}$]

References

1. Q. Huynh, A. Selmi, G. Corbel, P. Lacorre and J. Millet, *J. Catal.*, 2009, **266**, 64-70.
2. G. Mestl, T. Ilkenhans, D. Spielbauer, M. Dieterle, O. Timpe, J. Krohnert, F. Jentoft, H. Knzinger and R. Schlogl, *Appl. Catal. A: Gen.*, 2001, **210**, 13-34.